Electronic Supplementary Material (ESI) for Sustainable Energy & Fuels.

Positive self-reconstruction in FeNiMo phosphide electrocatalyst for enhanced overall water splitting

Yi Wei, Cheol-Hwan Shin, Gyan-Barimah Caleb, Emmanuel Batsa Tetteh, Gisang Park, Jong-Sung Yu*.

Department of Energy Science and Engineering, Daegu Gyeongbuk Institute of Science and Technology (DGIST), 333 Techno Jungang Daero, Hyeonpung-Myeon, Dalseong-Gun, Daegu 42988, Republic of Korea.

*Corresponding author: jsyu@dgist.ac.kr

Experimental

Materials preparation

Before preparation, a piece of NF was soaked into 0.5 M HCl for 5 min to remove the surface impurity layer and then cleaned with DI water and aceton for several times. Firstly, 0.5 mmol nickel chloride hexahydrate ($NiCl_2 \cdot 6H_2O$), 0.5 mmol iron chloride hexahydrate ($FeCl_3 \cdot 6H_2O$), and 0.5 mmol sodium molybdate dihydrate ($Na_2MoO_4 \cdot 6H_2O$) were dissolved into 10 mL DI water under a vigorous magnetic stirring. Then, the cleaned Ni foam was kept into the suspension and treated under ultrasonication for 3 min. Next, the immersed NF was taken out and dried at 70 °C for 5 h, before thermal phosphidation of the dried NF under argon gas at 350 °C for 1 h to form FeNiMoP sample. In details, 1.0 g sodium hypophosphite monohydrate as phosphorus source was put upstream while the dried nickel foam was placed downstream. Then, the sample was collected after cooled down to room temperature. The same method was employed for the preparation of NiMoP, FeMoP, and FeNiP except with the absence of $FeCl_3 \cdot 6H_2O$, $NiCl_2 \cdot 6H_2O$ and $Na_2MoO_4 \cdot 6H_2O$, respectively. All the catalyst loading was maintained at 1.0 mg cm^{-2}.

The IrO_2/NF sample was prepared as follows: 40 mg of IrO_2 was mixed with 800 µL water, 175 µL isopropanol, and 25 µL Nafion (5%) in a 5 mL glass vial, and then under sonication treatment for 2 h to form a brown slurry. And then, the surface cleaned NF was dipped in the slurry and then taken out and dried at 70 °C for 5 h (Catalyst loading was around 1 mg cm^{-2}). The cathodic electrode (Pt/C)/NF was prepared in a similar way to the IrO_2/NF. In short, 5 mg commercial Pt/C (20% purchased from TANAKA company) mixed with 800 µL water, 175 µL isopropanol, and 25 µL Nafion in a 5 mL glass vial followed by ultrasonication for 2 h to get a black slurry. Then 10 µL of as-prepared ink dropped on a cleaned NF (5 mm × 5 mm), and then dried in an oven at 70 °C for 2 h. This process was repeated 4 times, making sure the catalyst loading was at 1 mg cm^{-2}.

Characterization

X-ray diffraction (XRD) was measured with a Rigaku Smartlab diffractometer with Cu-Kα (0.15406 nm). X-ray photoelectron spectroscopy (XPS) was operated on an AXIS-NOVA (Kratos). The scanning electron microscopy (SEM) was measured using a Hitachi S-4700 microscope. The transmission electron microscope (TEM), and scanning TEM (STEM), as well as energy dispersive X-ray spectroscopy (EDS) profile and elemental mapping were

conducted on Hitachi HF-3300. Raman spectroscopy was obtained on the Nicolet Almega XR Raman microscope under an excitation of 532 nm laser. The in-situ Raman spectra experiment were conducted with a potentiostat (Biologic VMP3), using a homemade electrolytic cell with a quartz glass as the cover to protect the objective. Pt wire, $Ag/AgCl_{(Sat. KCl)}$, and FeNiMoP/NF were employed as counter electrode, reference electrolyte, and working electrode, respectively. The plane of the working electrode was perpendicular to the incident laser.

Electrochemical measurements

The electrochemical characterizations were measured by a standard three-electrode system in N_2 satureted 1.0 M KOH on a potentiostat (Biologic VMP3). The $Ag/AgCl_{(Sat.KCl)}$, Platinum wire and the as-prepared catalysts loaded on NF were used as the reference electrode, counter electrode, and working electrode, respectively. The cyclic voltammetry (CV) curves were obtained by applying a scan rate of 50 mV s^{-1}. The LSV polarization curves were obtained with a scan rate of 5 mV s^{-1} after CV test for 10 times. The electrochemical impedance spectroscopy (EIS) measurements were applied from the frequency of 100 kHz to 0.1 Hz. The chronopotentiometry was conducted at 10 mA cm^{-2} in the 1.0 M KOH solution. The double-layer capacitance (C_{dl}) values were evaluated by performing CV measurements at the scan rates from 20 mV s^{-1} to 100 mV s^{-1} in a potentials range from 1.024 V to 1.124 V vs RHE. All electrode potentials in this work were converted into the reversible hydrogen electrode (RHE) using the following equation: $E_{RHE} = E_{Ag|AgCl} + 0.197\ V + 0.059pH$. 85% IR drop was compensated through the positive feedback model.

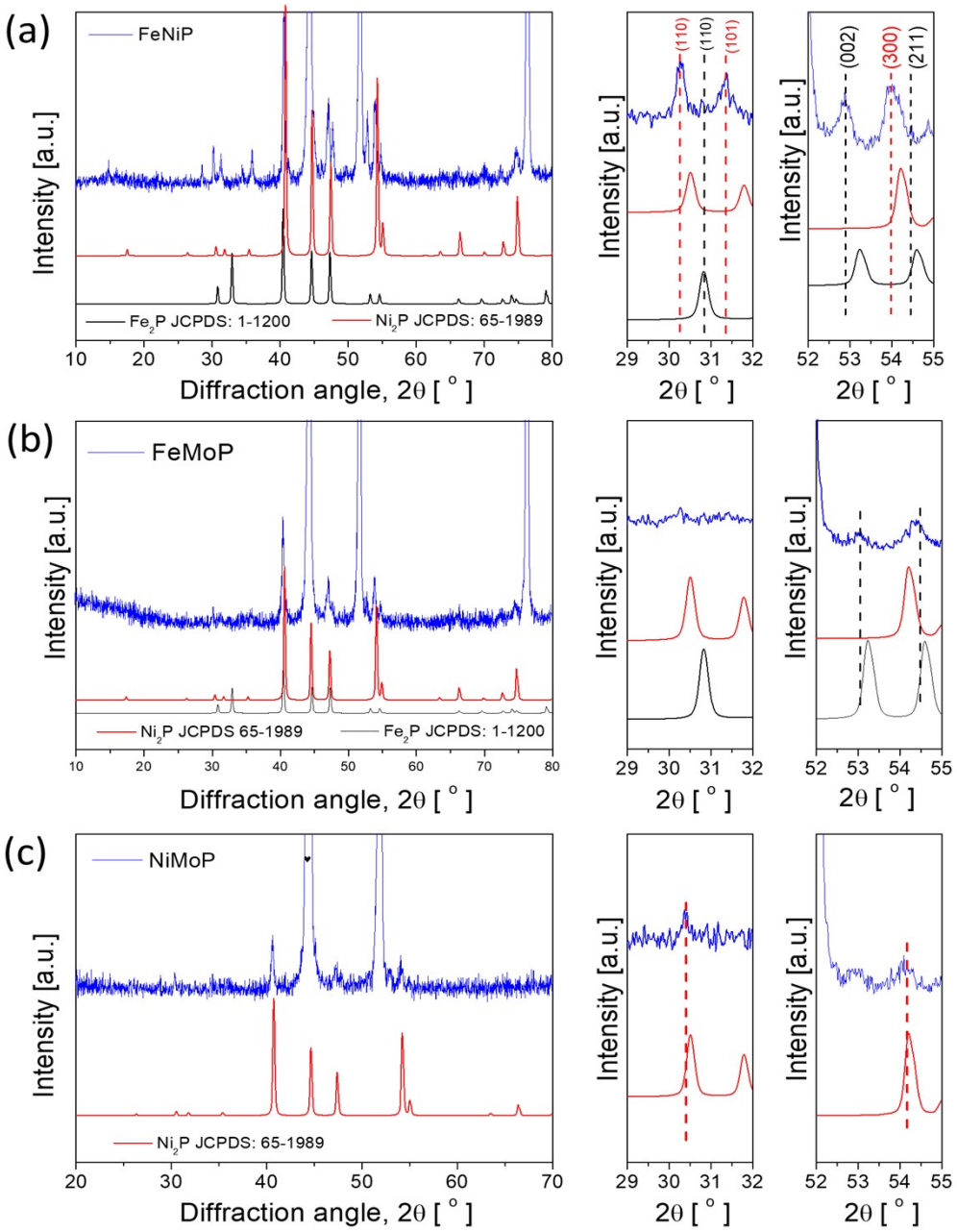

Fig. S1 XRD patterns of (a) FeNiP, (b) FeMoP and (c) NiMoP.

Table S1 The values showing the difference between the peak position angles of as-prepared samples and the corresponding reference diffraction angles for various diffraction planes.

Sample	(110) Ni_2P	(110) Fe_2P	(101) Ni_2P	(002) Fe_2P	(300) Ni_2P	(211) Fe_2P
FeNiMoP	0.21°	0°	0.37°	0.27°	0.21°	0.28°
FeNiP	0.24°	–	0.40°	0.32°	0.21°	0.14°
FeMoP	–	–	–	0.16°	–	0.10°
NiMoP	0.08°	–	–	–	0.08°	–

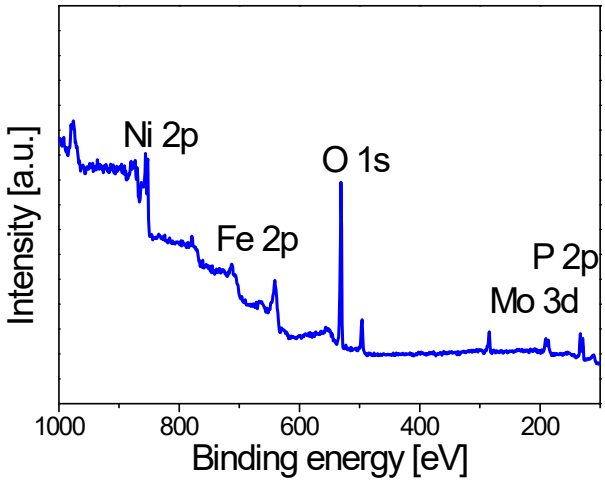

Fig. S2 XPS survey spectrum of as-prepared FeNiMoP.

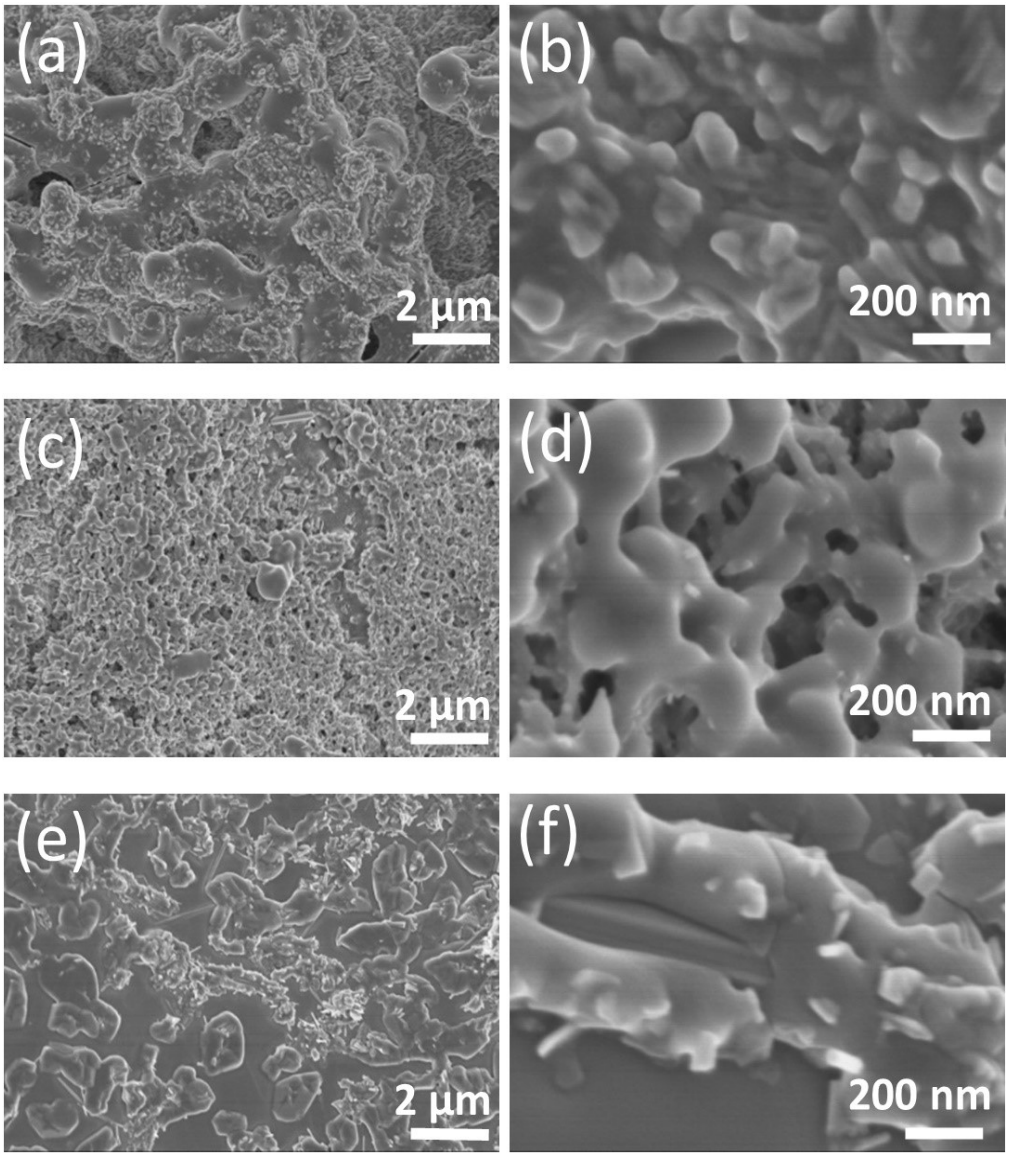

Fig. S3 SEM images of (a-b) FeNiP, (c-d) FeMoP and (e-f) NiMoP.

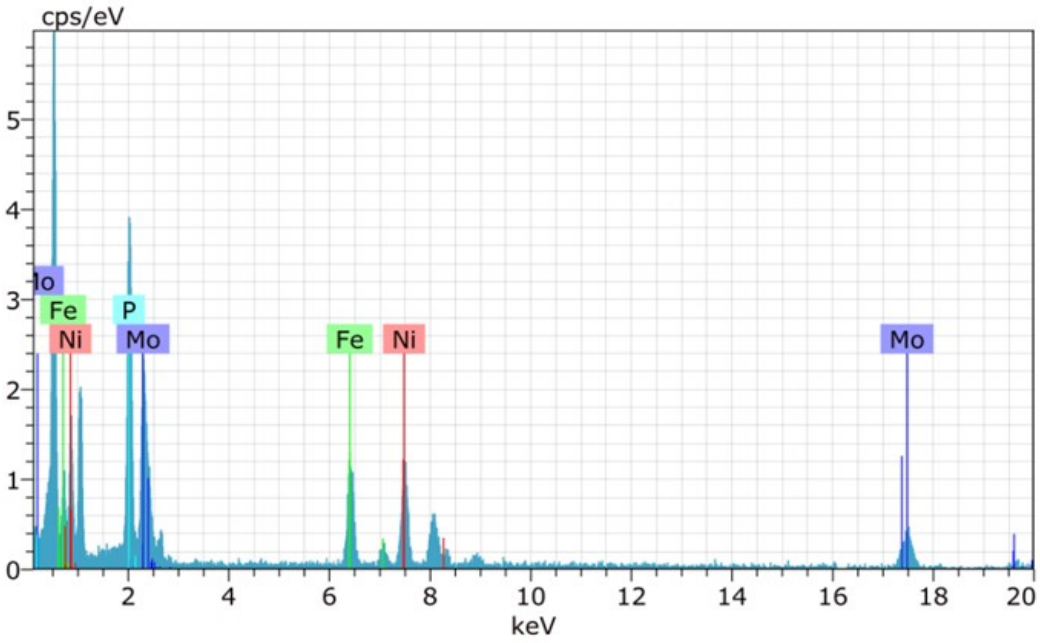

Spectrum: 1

Element	Series	unn. C [wt.%]	norm. C [wt.%]	Atom. C [at.%]	Error (3 Sigma) [wt.%]
Nickel	K-series	16.88	16.88	15.65	2.15
Iron	K-series	15.92	15.92	15.50	2.01
Molybdenum	L-series	41.35	41.35	23.45	12.78
Phosphorus	K-series	25.85	25.85	45.40	2.82
	Total:	100.00	100.00	100.00	

Fig. S4 EDS profile and corresponding elemental composition of Ni, Fe, Mo, and P from as-prepared FeNiMoP.

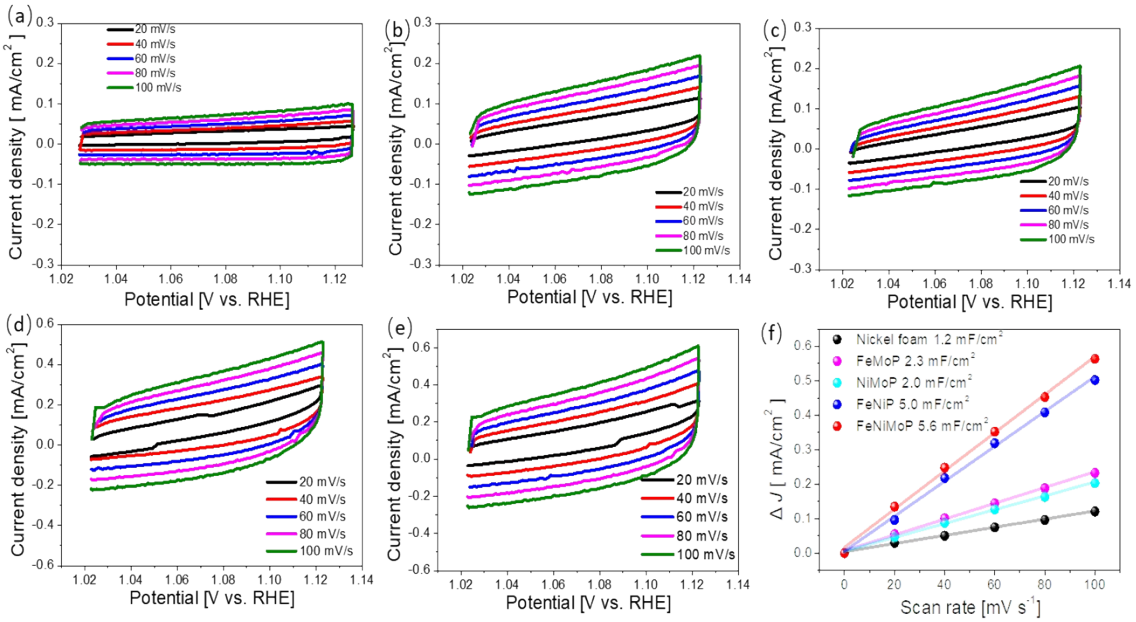

Fig. S5 (a) Cyclic voltammetry curves of (a) NF, (b) FeMoP, (c) NiMoP, (d) FeNiP and (e) FeNiMoP at the scan rates from 20 to 100 mV s^{-1} with a 20 mV s^{-1} interval in the potential range from 1.024 V to 1.124 V vs RHE. (f) Plots showing the dependence of current density on the scan rate for the extraction of double-layer capacitance (C_{dl}) performed on NF, FeMoP, NiMoP, FeNiP and FeNiMoP.

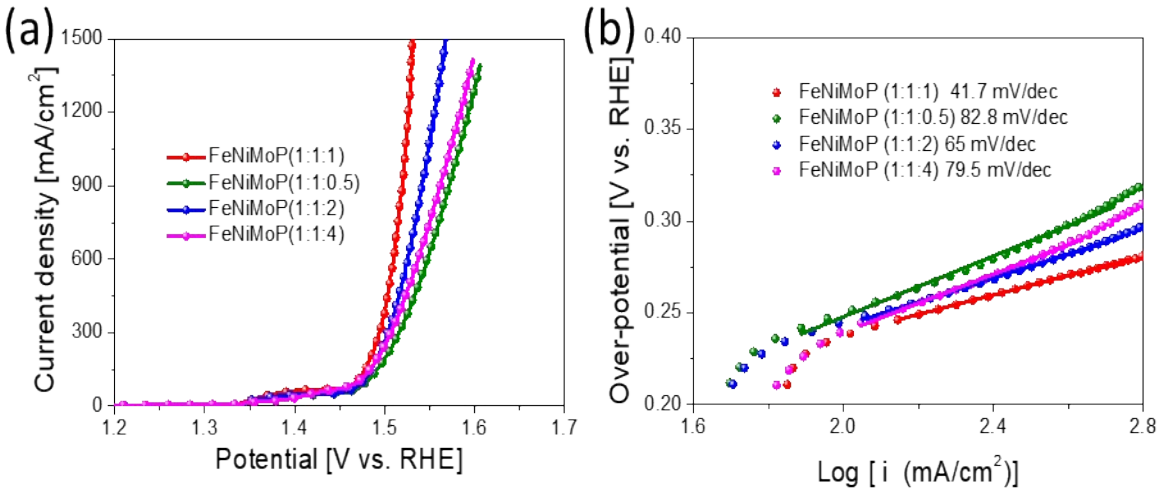

Fig. S6 (a) OER polarization curves and (b) the corresponding Tafel slopes of FeNiMoP catalysts with different MoP mole ratios performed in 1.0 M KOH electrolyte.

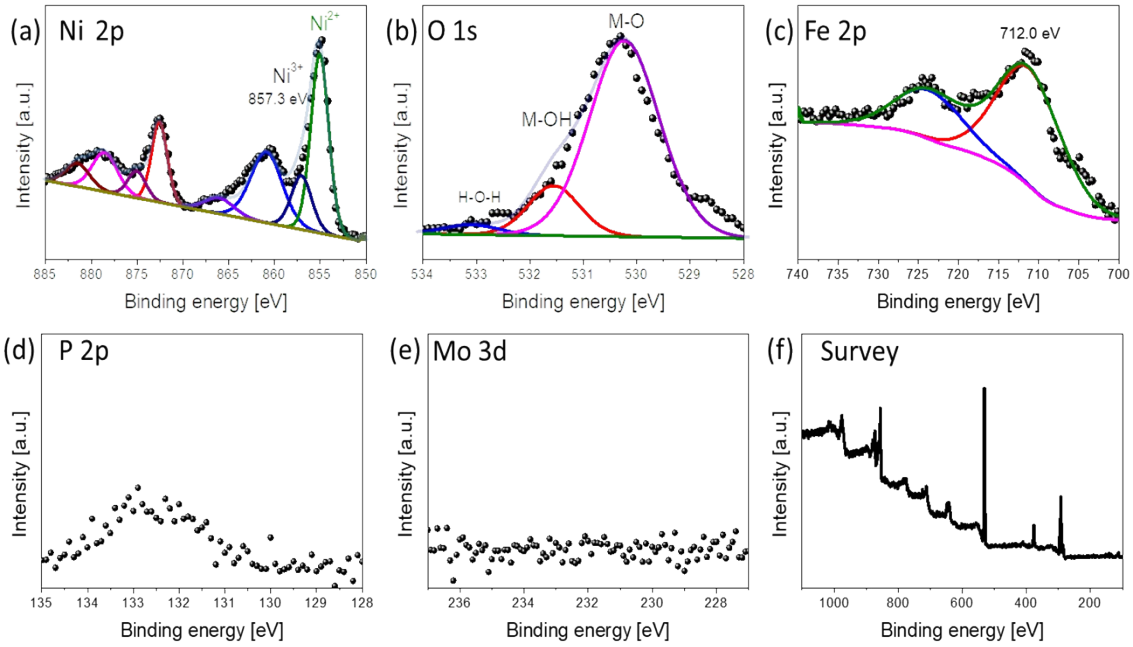

Fig. S7 High-resolved XPS spectra of (a) Ni 2p, (b) O1s, (c) Fe 2p, (d) P 2p, and (e) Mo 3d of FeNiMoP after long-term OER stability test in Fig. 3b. (f) Corresponding XPS survey of FeNiMoP after the stability test.

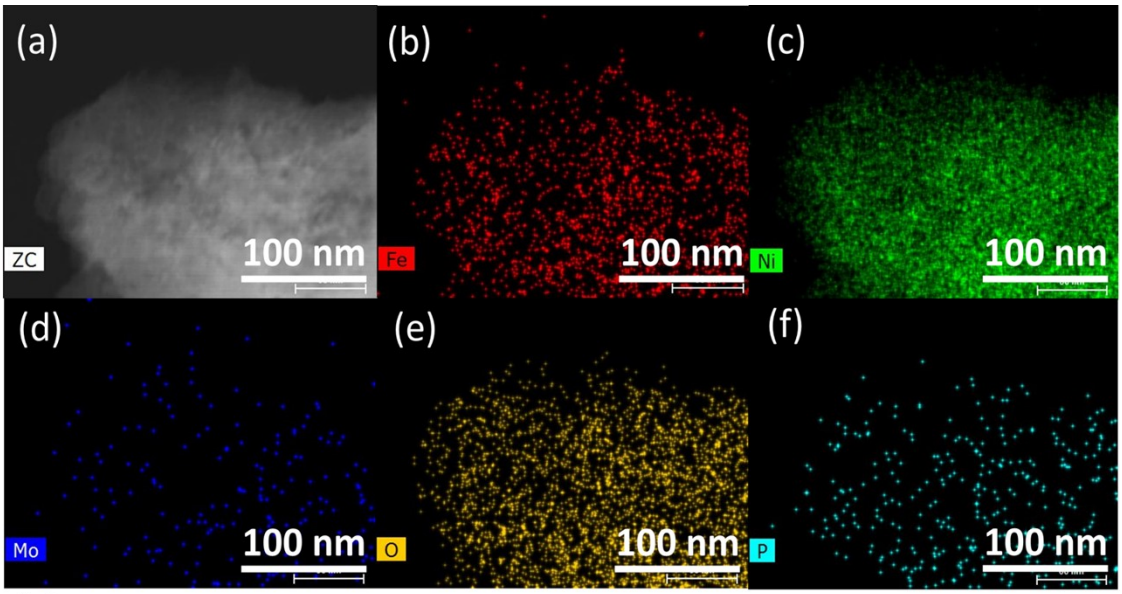

(g)

Spectrum: 1

Element	Series	unn. C [wt.%]	norm. C [wt.%]	Atom. C [at.%]	Error (3 Sigma) [wt.%]
Iron	K-series	3.79	3.79	2.94	1.11
Nickel	K-series	82.74	82.74	61.09	8.92
Molybdenum	L-series	0.00	0.00	0.00	0.00
Phosphorus	K-series	0.38	0.38	0.54	0.35
Oxygen	K-series	13.08	13.08	35.43	2.50
	Total:	100.00	100.00	100.00	

Fig. S8 STEM images of FeNiMoP after long-term OER stability test in Fig. 3b and corresponding element mapping images of (b) Fe, (c) Ni, (d) Mo, (e) O, and (f) P elements. (g) Summary of elemental composition based on the EDS-mapping.

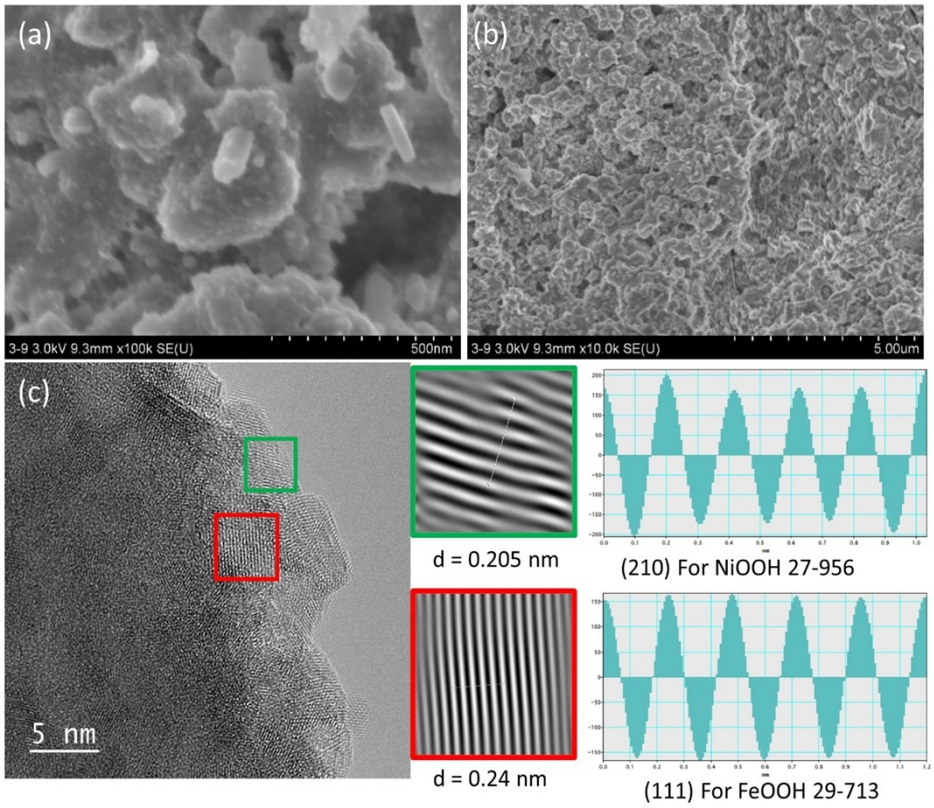

Fig. S9 (a) and (b) SEM images at different magnification and (c) corresponding HR-TEM image of FeNiMoP after long-term OER test in Fig. 3b.

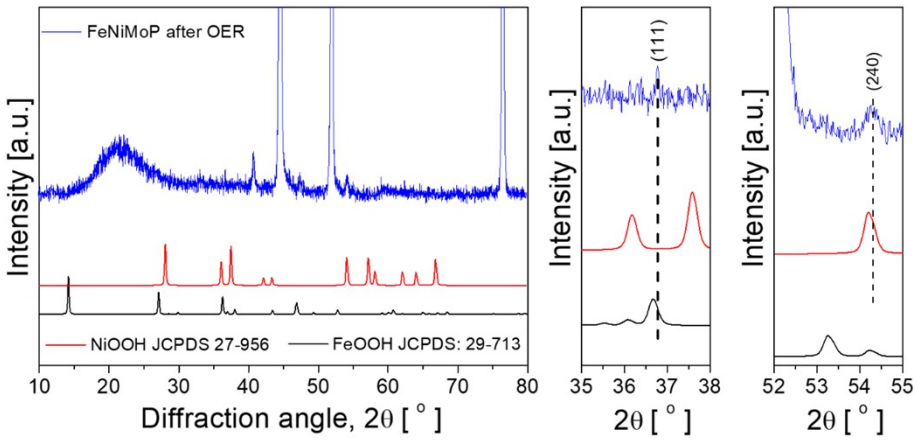

Fig. S10 XRD patterns of FeNiMoP after OER stability test in Fig. 3b.

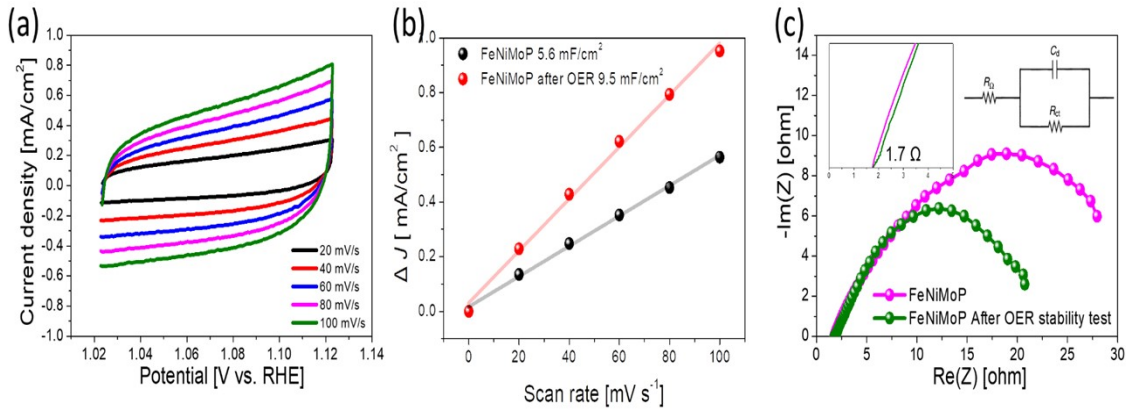

Fig. S11 (a) Cyclic voltammetry curves of FeNiMoP after long-term OER stability test in Fig. 3b at different rates from 20 to 100 mV s-1 with a 20 mV s^{-1} interval in the potential range from 1.024 V to 1.124 V vs RHE. (b) Capacitive $\triangle$J (= $J_a - J_c$) versus the scan rates and (c) Nyquist plots of FeNiMoP before and after the stability test.

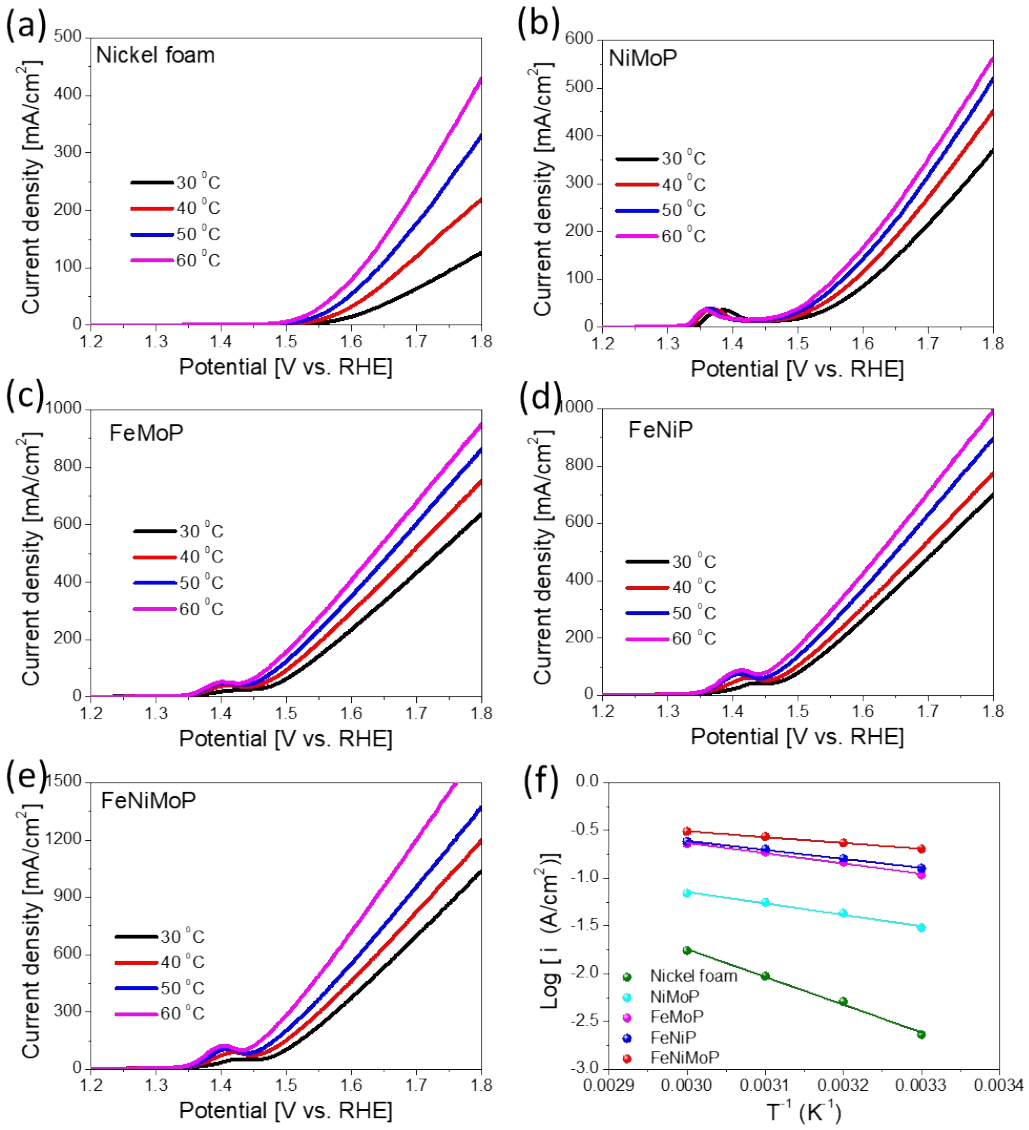

Fig. S12 OER polarization curves tested at different temperature (without IR correction) for (a) bare nickel foam, (b) NiMoP, (c) FeMoP, (d) FeNiP, and (e) FeNiMoP in 1.0 M KOH with the scan rate of 2.0 mV s^{-1} at 30 °C, 40 °C, 50 °C, 60 °C, respectively. (f) Arrhenius plots of the current density at the overpotential of 300 mV without iR correction

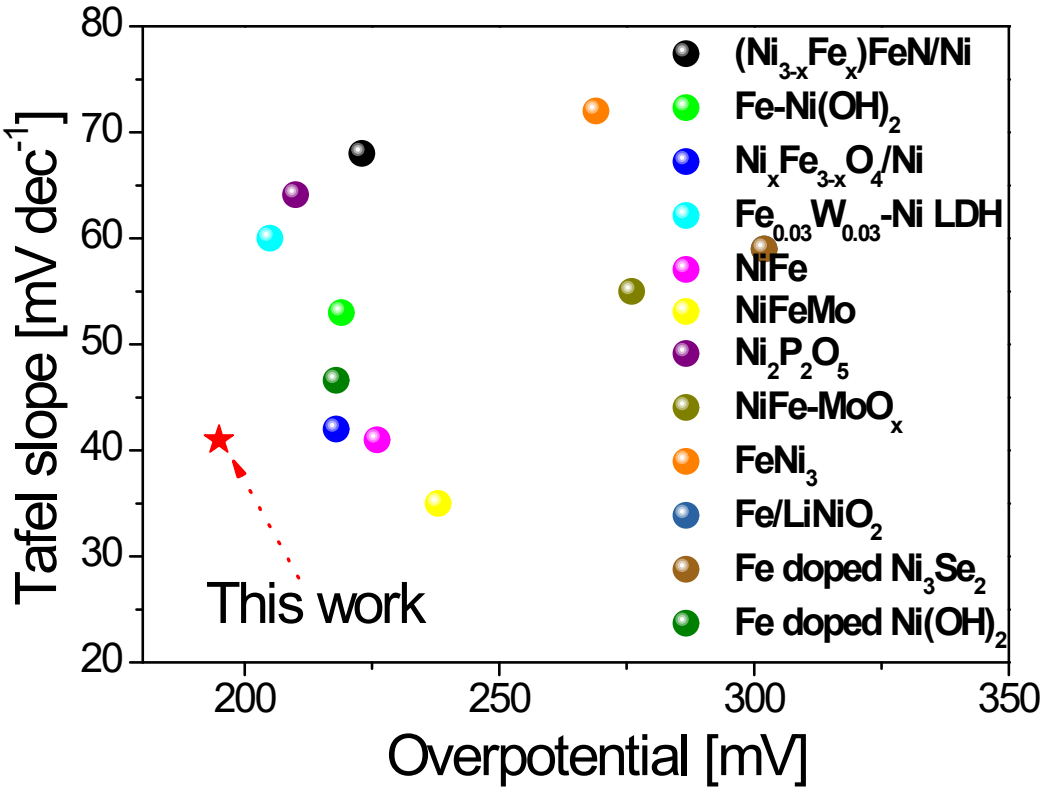

Fig. S13 Comparison with recently reported FeNi-based OER electrocatalyst references: $(Ni_{3-x}Fe_x)FeN/Ni$,[1] $Fe\text{-}Ni(OH)_2$,[2] $Ni_xFe_{3-x}O_4/Ni$,[3] $Fe_{0.03}W_{0.03}$-Ni,[4] NiFe alloy,[5] NiFeMo,[6] $Ni_2P_2O_7$,[7] $NiFe\text{-}MoO_x$,[8] $FeNi_3$,[9] $Fe/LiNiO_2$,[10] Fe-doped Ni_3Se_2,[11] Fe-doped β-$Ni(OH)_2$.[12]

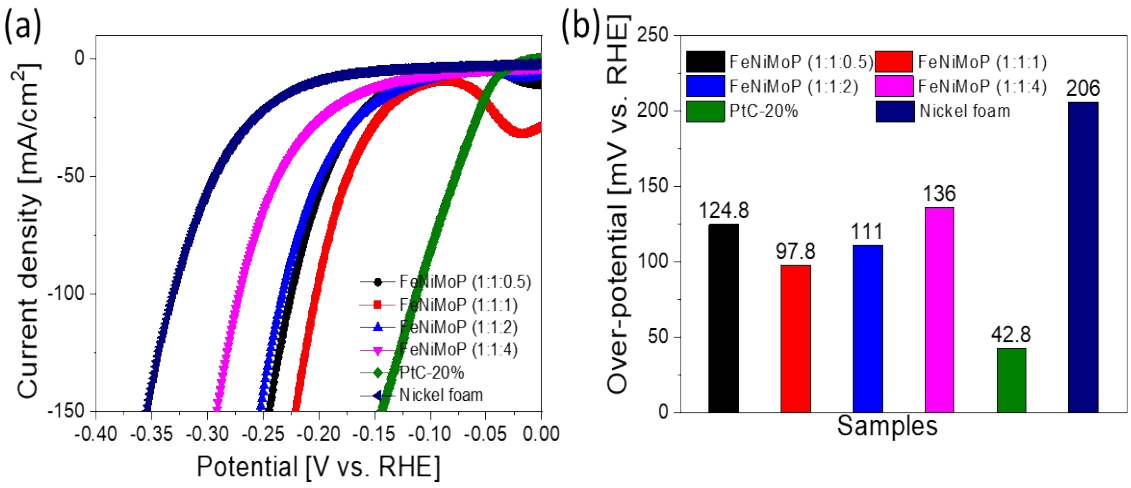

Fig. S14 (a) HER polarization curves and (b) their corresponding overpotentials at 10 mA/cm^2 of FeNiMoP catalysts with different mole ratios of MoP.

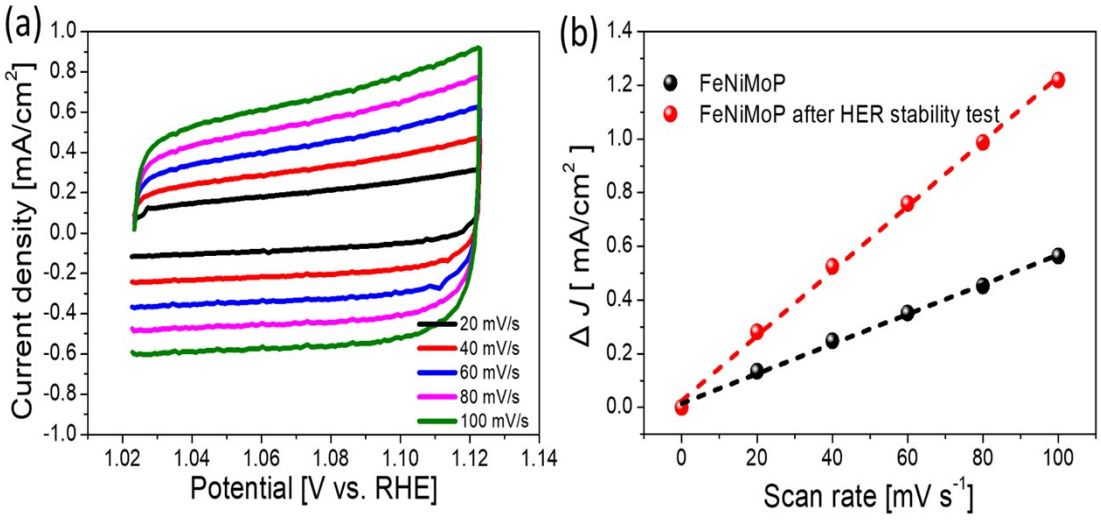

Fig. S15 (a) Cyclic voltammetry curves of FeNiMoP after HER stability test in Fig. 4c at different rates from 20 to 100 mV s^{-1} with a 20 mV s^{-1} interval in the potential range from 1.024 V to 1.124 V vs RHE. (b) Capacitive $\triangle$J (= $J_a - J_c$) versus the scan rates of FeNiMoP before and after the HER stability test.

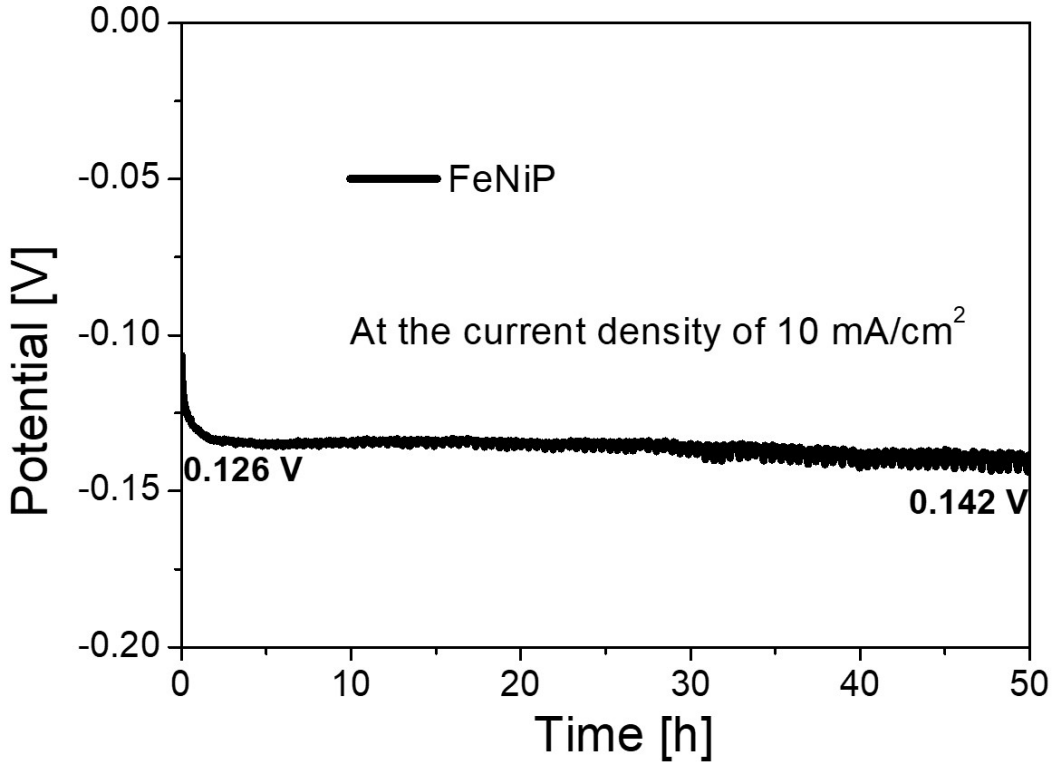

Fig. S16 HER long-term stability test of FeNiP at the current density of 10 mA cm^{-2}.

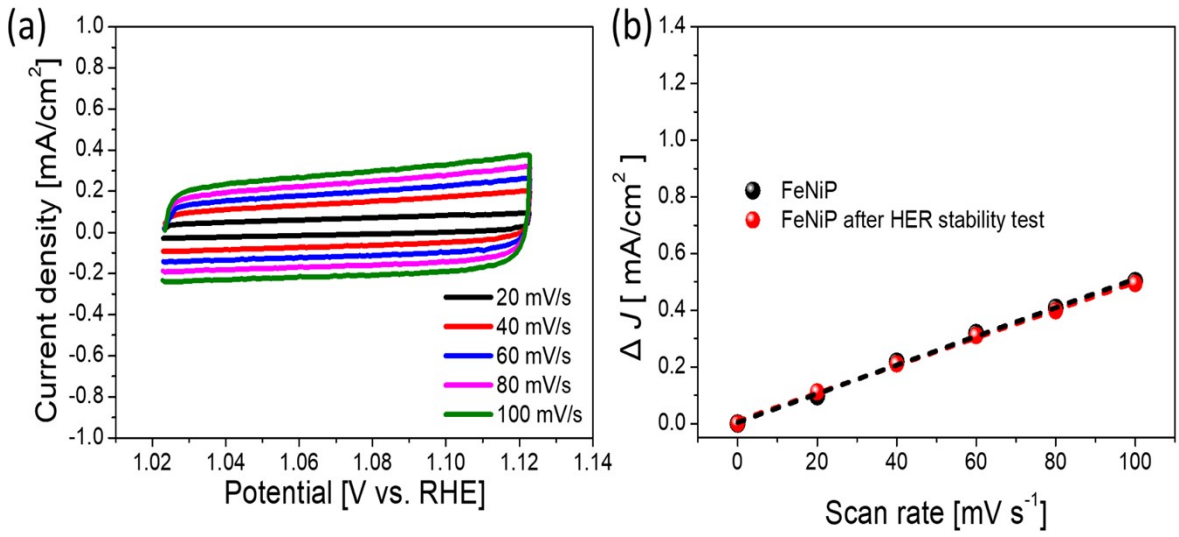

Fig. S17 (a) Cyclic voltammetry curves of FeNiP after HER stability test in Fig. S16 at different rates from 20 to 100 mV s^{-1} with a 20 mV s^{-1} interval in the potential range from 1.024 V to 1.124 V vs RHE. (b) Capacitive $\triangle$J (= $J_a - J_c$) versus the scan rates of FeNiP before and after the HER stability test.

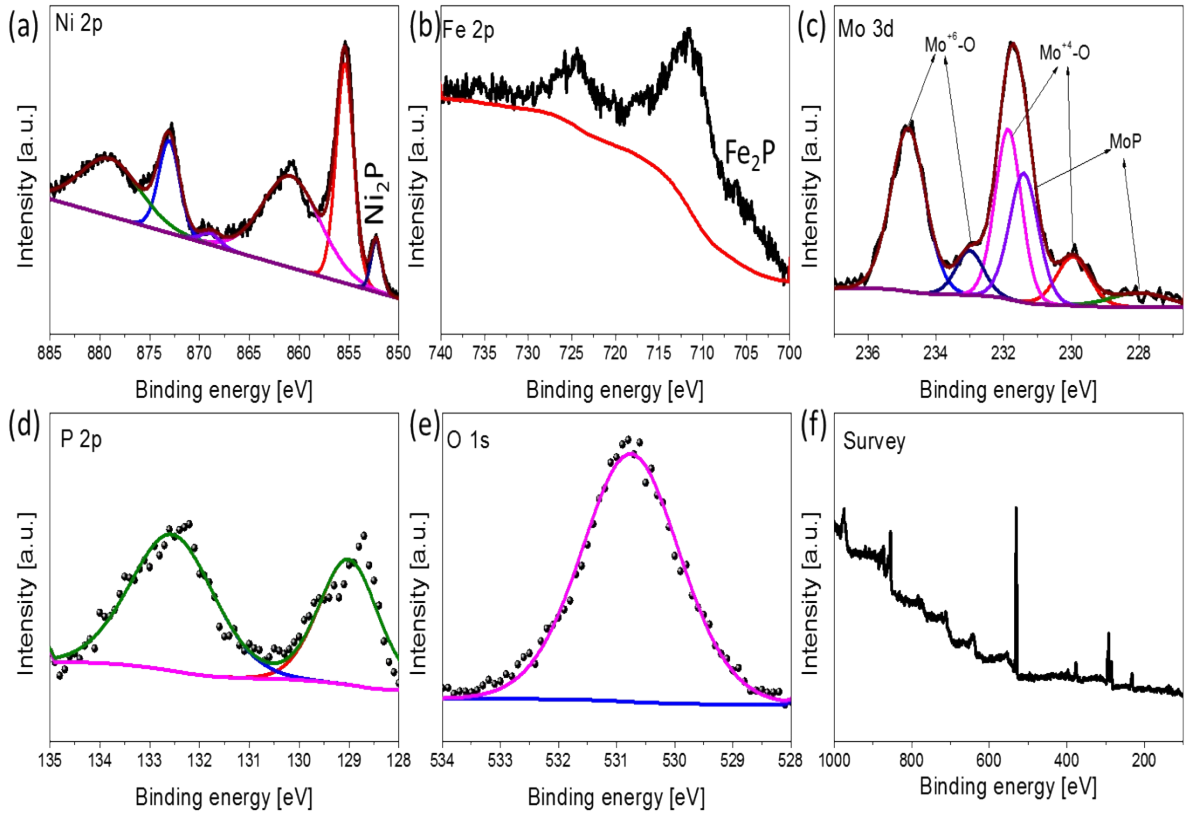

Fig. S18 XPS profiles of FeNiMoP after long-term HER stability test in Fig. 4c, (a) Ni 2p, (b) Fe 2p, (c) Mo 3d, (d) P 2p, (e) O 1s and (f) corresponding survey scan.

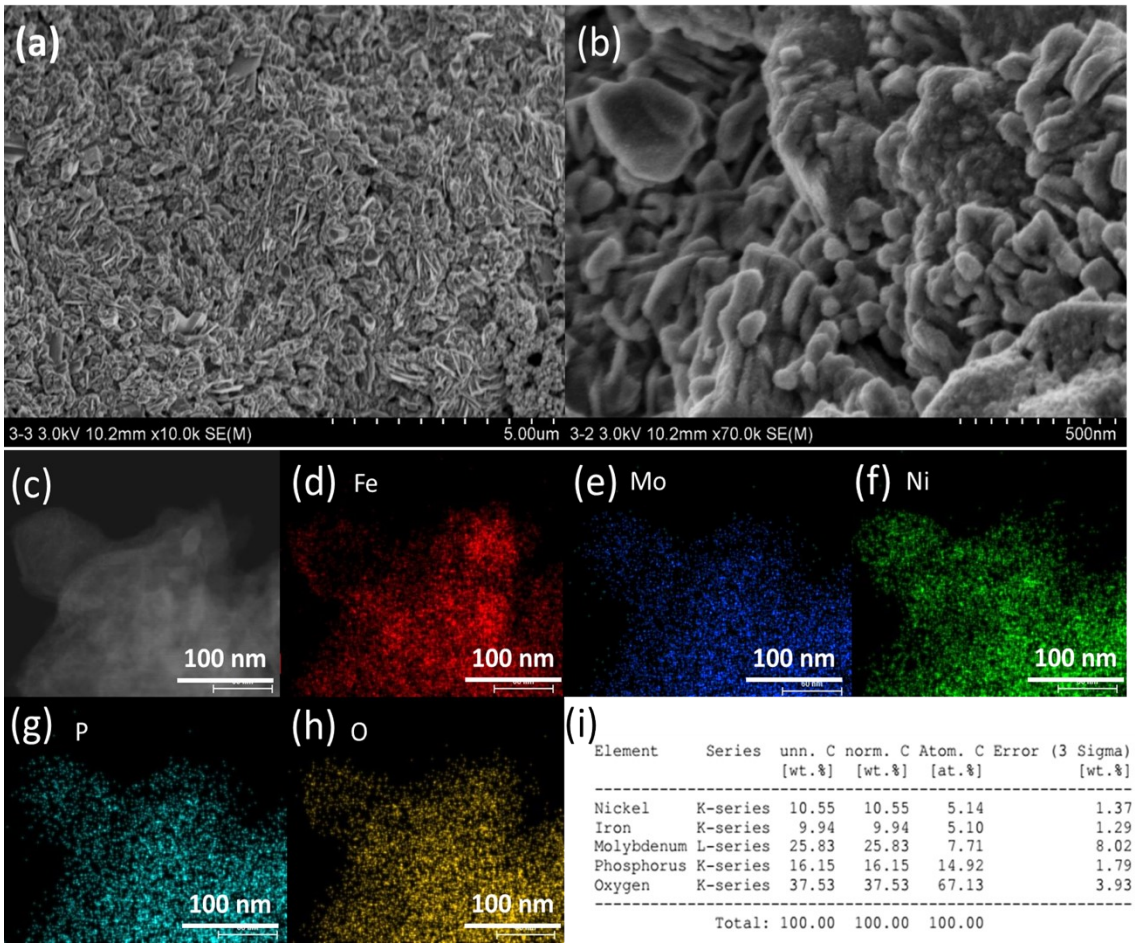

Element	Series	unn. C [wt.%]	norm. C [wt.%]	Atom. C [at.%]	Error (3 Sigma) [wt.%]
Nickel	K-series	10.55	10.55	5.14	1.37
Iron	K-series	9.94	9.94	5.10	1.29
Molybdenum	L-series	25.83	25.83	7.71	8.02
Phosphorus	K-series	16.15	16.15	14.92	1.79
Oxygen	K-series	37.53	37.53	67.13	3.93
	Total:	100.00	100.00	100.00	

Fig. S19 (a) and (b) SEM images, (c) STEM image and corresponding element mapping images of (d) Fe, (e) Mo, (f) Ni, (g) P, (h) O, and (i) summary of the elemental composition of FeNiMoP after HER stability test in Fig. 4c.

REFERENCES

1 M. Yan, K. Mao, P. Cui, C. Chen, J. Zhao, X. Wang, L. Yang, H. Yang, Q. Wu and Z. Hu, *Nano Res.*, 2020, **13**, 328–334.

2 T. Kou, S. Wang, J. L. Hauser, M. Chen, S. R. J. Oliver, Y. Ye, J. Guo and Y. Li, *ACS Energy Lett.*, 2019, **4**, 622–628.

3 D. Li, S. Liu, G. Ye, W. Zhu, K. Zhao, M. Luo and Z. He, *Green Chem.*, 2020, **22**, 1710–1719.

4 C. Li, P. Tian, H. Pang, W. Gong, J. Ye and G. Ning, *Sustain. Energy Fuels*, 2020, **4**, 2792–2799.

5 C. Wang, H. Yang, Y. Zhang and Q. Wang, *Angew. Chemie Int. Ed.*, 2019, **58**, 6099–6103.

6 F. Qin, Z. Zhao, M. K. Alam, Y. Ni, F. Robles-Hernandez, L. Yu, S. Chen, Z. Ren, Z. Wang and J. Bao, *ACS Energy Lett.*, 2018, **3**, 546–554.

7 S. Surendran, A. Sivanantham, S. Shanmugam, U. Sim and R. Kalai Selvan, *Sustain. Energy Fuels*, 2019, **3**, 2435–2446.

8 C. Xie, Y. Wang, K. Hu, L. Tao, X. Huang, J. Huo and S. Wang, *J. Mater. Chem. A*, 2017, **5**, 87–91.

9 J. Ding, Q. Sun, L. Zhong, X. Wang, L. Chai, Q. Li, T. T. Li, Y. Hu, J. Qian and S. Huang, *Electrochim. Acta*, 2020, **354**, 136716.

10 K. Zhu, T. Wu, Y. Zhu, X. Li, M. Li, R. Lu, J. Wang, X. Zhu and W. Yang, *ACS Energy Lett.*, 2017, **2**, 1654–1660.

11 M. Ghaemmaghami, Y. Yamini, E. Saievar-Iranizad and A. Bayat, *Sustain. Energy Fuels*, 2020, **4**, 1150–1156.

12 X. Qiao, H. Kang, Y. Li, K. Cui, X. Jia, H. Liu, W. Qin, M. Pupucevski and G. Wu, *ACS Appl. Mater. Interfaces*, 2020, **12**, 36208–36219.